Journal of Nuclear Materials 467 (2015) 418–423

Contents lists available at ScienceDirect

Journal of Nuclear Materials

journal homepage: www.elsevier.com/locate/jnucmat

Migration of rhenium and osmium interstitials in tungsten

Tomoaki Suzudo [a, *], Masatake Yamaguchi [a], Akira Hasegawa [b]

[a] Center for Computational Science and e-Systems, Japan Atomic Energy Agency, 2-4 Shirane Shirakata, Tokai-mura, 319-1195, Japan
[b] Department of Quantum Science and Energy Engineering, Tohoku University, 6-6-01-2 Aramaki-aza-Aoba, Aoba-ku Sendai, 980-8579, Japan

HIGHLIGHTS

- We investigate the migration of rhenium and osmium in tungsten.
- The low rotation barrier of mixed dumbbells greatly influences their diffusivities.
- One cannot reduce their migration behavior to that of spherical objects.

ARTICLE INFO

Article history:
Received 13 February 2015
Received in revised form
18 May 2015
Accepted 19 May 2015
Available online 3 June 2015

Keywords:
Kinetic Monte Carlo method
Rhenium and osmium in tungsten
Migration
Diffusivity
Radiation induced precipitates

ABSTRACT

Tungsten is expected to be a promising plasma-facing material for future fusion devices, but radiation-induced precipitation (RIP), which leads the material to hardening, is a concern at their practical use. One of the keys to accurate prediction of the emergence of RIP is migration of solute atoms, rhenium and osmium, that are produced by nuclear transmutation through irradiation. We conduct a series of numerical simulations using an atomic kinetic Monte Carlo method and investigate the migration of these solute atoms in the form of tungsten–rhenium and tungsten–osmium mixed dumbbells, considered to be the most efficient "carriers" of the solute atoms. We find that the low rotation energy barrier of these mixed dumbbells leading to three-dimensional migration greatly influences their diffusivities. The result also suggests that, although these dumbbells have three-dimensional motion, one cannot simply reduce their migration behavior to that of vacancy-like spherical objects.

1. Introduction

Due to its high melting point and good resistance to sputtering, tungsten (W) is a promising candidate material for high-temperature and heavy irradiation applications, e.g. for the first wall and the diverter armor of nuclear fusion devices of the future. See, for example, Ref. [1] for information regarding recent developments of W materials for fusion applications.

Under neutron irradiation, transmutation elements are produced in W [2,3]. Among them, rhenium (Re) and osmium (Os) are the two main products; Os is produced via the production of Re. According to a predictive estimation [3], pure W used for the first wall armor of a nuclear fusion device is transmuted to an end-of-service alloy composition of approximately 91 at.% W, 6 at.% Re, and 3 at.% Os.

It is widely known that Re and Os precipitate under irradiation with solute concentrations below their solid solubility limits [4–10] which, at room temperature, are ~27 at.% and ~5 at.% for Re and Os, respectively [11,12]. This is a common radiation effect, observed in many alloys, and is known as radiation-induced precipitation (RIP). Because incoherent precipitates become obstacles for dislocation motions and are responsible for radiation hardening [9,13] that can lead to embrittlement of the materials, nucleation and growth of RIP under the fusion reactor environment must be accurately predicted.

As well as nuclear transmutations, direct effects of irradiation of materials are atomic displacements, i.e., vacancies, self-interstitial atoms (SIAs) and their clusters. The emergence of RIP is roughly explained as follows: an SIA is binding a solute atom; a vacancy is binding another solute atom; then SIA-vacancy recombination can cause aggregation of solute atoms [14–16]. See Fig. 1 for the schematic picture of the RIP nucleation mechanism. Obviously, point defects produced by atomic displacements (i.e., vacancy and SIA) and solute atoms (Re and Os) are all attractive in W crystals. As an aggregated solute atom cannot be dissociated from others without the actions of 'carriers' such as vacancies and interstitial atoms, the

* Corresponding author.
E-mail address: suzudo.tomoaki@jaea.go.jp (T. Suzudo).

http://dx.doi.org/10.1016/j.jnucmat.2015.05.051
0022-3115/

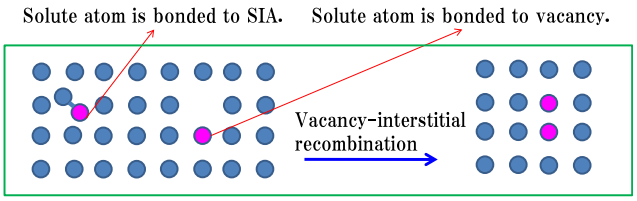

Fig. 1. RIP development mechanism; how solute atoms are aggregated [14].

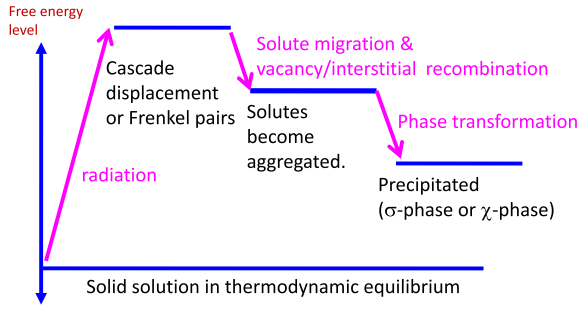

Fig. 2. Free energy changes over the process of RIP development.

clusters of solute atoms have long lives, giving them a chance to become large enough to be transformed into a different phase, such as σ-phase or χ-phase [8]. These precipitates are not in thermal equilibrium if the solute concentration is below the solid solubility limit. In other words, the free energy stored in a system having precipitates is larger than a system with Re, or Os, in solution. Because of this, the emergence of the RIP seems to be at odds with intuitive physical understanding, because the system seemingly gains the energy by itself. This is explained as follows: The free energy of the system is increased when the radiation produces atomic displacements; the system then loses the free energy when an interstitial atom and a vacancy recombine. The diagram in Fig. 2 illustrates this.

An additional atomistic phenomenon is necessary for the emergence of RIP, that is, migration of the solute atoms. The migration of Re and Os atoms in W plays a critical role in the development of RIP. The migration of solute atoms via the vacancy mode occurs through an exchange of a vacancy and an atom. In addition, a vacancy is able to drag a solute atom along with it if the solute atom and the vacancy are attractive to each other [17,18]. The migration style of solute atoms dragged by interstitials is more complicated, as there exist many types of interstitial atoms, located in tetrahedral or octahedral sites, or they exist as dumbbells with choices of various directions. As shown later in this paper, the migration of solutes via the interstitial mode are much faster than migration via the vacancy mode, and we believe that the interstitial migration mode would be the greater contributor to the aggregation of solute atoms.

In the current study, we aimed at investigating the migration of solute atoms via interstitial mode in W crystals by exploiting an atomic kinetic Monte Carlo method parameterized by the first principles studies [19]. We particularly focused upon the influence of the rotation energy barriers upon the migration of mixed dumbbells, as our previous study [19] suggests that their low rotation energy barriers leading to three-dimensional migration is key in the explanation of the radiation effect experimentally observed in W crystals.

Table 1
Formation energies of Re and Os interstitials in W (eV).

Interstitial-type	SIA	Re-interstitial	Os-interstitial
<111> crowdion	9.77	9.29	6.11
<111> dumbbell	9.78	9.17	5.84
<110> dumbbell	10.21	9.20	5.68
Tetrahedral interstitial	11.38	10.53	6.90
<100> dumbbell	11.86	10.20	7.79
Octahedral interstitial	11.97	11.32	8.11

2. Methodology

2.1. Energetics of point defects and solute atoms

The first principles studies necessary to the current study are conducted in the framework of generalized gradient approximation with projector-augmented wave pseudo-potentials [20] using the Vienna *ab initio* simulation package (VASP) [21]. The detail is reported in Ref. [19], and we use its results in the following. Table 1 and Fig. 3 summarize formation energy of SIA, Re interstitials, and Os interstitials in various forms. According to these results, the most energetically-favored forms for SIA, Re-interstitial, Os-interstitial are <111> dumbbell, <111> dumbbell and <110> dumbbell, respectively. Note that in the current paper, we use the expressions, <111> crowdion, and <111> dumbbell, interchangeably. For SIA and Re interstitials, some *ab initio* studies reported that asymmetric directions <11h> (h ~ 0.5) are slightly more favored than <111> dumbbells [19], but we do not know whether these asymmetric dumbbells are realistic. In addition, excess formation energies of <111> dumbbells from <11h> are not large, being equal to ~0.1 eV or less, so we consider <111> dumbbells as the most favored species for SIAs and Re interstitials in the current study.

Table 2 summarizes the binding energies between the solute atoms at a substitutional position and at point defects. Attractive relations are indicated for all the combinations. Note that in the current paper, it is assumed that a positive binding energy indicates attraction. This ensures that part of the conditions necessary for RIP development, described above, are satisfied. Since a vacancy and either of the Os and Re solute atoms are mutually attractive at the second nearest neighbor positions, vacancies are expected to drag the solute atoms.

Table 3 summarizes migration energy barriers of the solute atoms. It indicates that migrations via the vacancy mode are extremely slow compared with those via the interstitial mode. We believe that migrations via the interstitial mode carry the solute atoms much more effectively than do migrations via the vacancy mode and we, in the current paper, concentrate on the migration

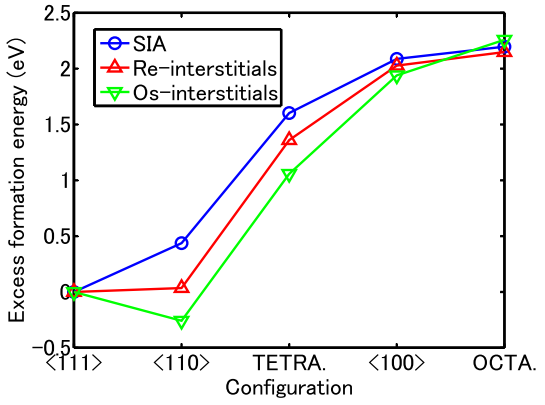

Fig. 3. Relative formation energy of SIAs and Re/Os interstitials in W crystals.

Table 2
Binding energy between the solute atoms at a substitutional position and point defects in W crystals (eV); values are calculated by *ab initio* studies [19]. "1NN" and "2NN" stand for the first and second nearest neighbors, respectively.

	Vacancy		SIA
	1NN	2NN	Mixed dumbbell
Re in W	0.22	0.22	0.79
Os in W	0.53	0.36	1.87

Table 3
Migration energy barriers of vacancy, SIA and solute atoms in W crystals (eV). For SIA and Re-interstitial, migration in the <111> direction is assumed. For Os interstitial, translation-and-rotation migration mode was considered.

Defect	Migration barrier (eV)
Vacancy	1.69
SIA	0.003
Re-substitutional	1.65
Os-substitutional	1.43
Re-interstitial	0.12
Os-interstitial	0.31

via interstitial mode.

Those events involving the solute interstitials that are to be considered in the AKMC are schematically depicted in Fig. 4 and Fig. 5 for Re-interstitials and Os-interstitials, respectively. Because the <111> dumbbell is the most favored for Re-interstitials, we consider a translation event in <111> directions, that is, the jump from Fig. 4a to b. For Os-interstitials, the <110> dumbbell is the most favored, and we consider translation-rotations event from one <110> dumbbell to another <110> dumbbell at the first nearest neighbor position, that is for example, the jump from Fig. 5a to b.

We also consider pure rotation events of each dumbbell; if the <111> dumbbell is the most favored, it is subject to change in direction to another <111> via a <110> direction, depicted as the change from Fig. 4b to c. In this case, the rotation energy barrier

Table 4
Rotation energy barriers of SIA and mixed dumbbell in W (eV).

Defect	Rotation path	Rotation barrier (eV)
SIA dumbbell	<111>→<110>→<111>	0.43
W–Re dumbbell	<111>→<110>→<111>	0.03
W–Os dumbbell	<110>→<111>→<110>	0.16

corresponds to the excess formation energy of the <110> dumbbell over that of the <111> dumbbell. If the <110> dumbbell is the most favored, it is subject to change in direction to another <110> via <111> direction, depicted as the change from Fig. 5b to c. In this case, the rotation energy barrier is equal to the excess energy of the <111> dumbbell over that of the <110> dumbbell. The rotation energy barrier of each dumbbell is calculated by *ab initio* method [19] and is shown in Table 4.

An obvious and important consequence of the set of events considered for W–Re mixed dumbbells is that they could not have migrated were the pure rotation event not allowed; the Re atom would have been trapped between two neighboring W atoms. This "immobility" can be easily demonstrated by an AKMC simulation. It is possible for a W–Re mixed dumbbell to be separated into a SIA and a Re atom at a substitutional site, but such a substitutional Re atom can move only slowly via the vacancy mode, as the migration energy barrier is large (See Table 3). Thus, the pure rotation event is essential to the ease of migration of Re atoms in W crystals, in turn making it essential to the emergence of RIP in W–Re alloys.

2.2. Atomic kinetic Monte Carlo method

In this subsection, the detail of the AKMC method used in the present study is explained. First, we create a perfect W bcc crystal with the dimension of $20a_0 \times 20a_0 \times 20a_0$, where a_0 is 3.169 Å, the lattice constant of W crystals; a_0 is estimated by a set of *ab initio* calculations [22]. Second, we insert an extra atom into the perfect crystal. The inserted atom is W, Re or Os, and this defect becomes an SIA (<111> dumbbell), a Re-interstitial (<111> mixed dumbbell), or

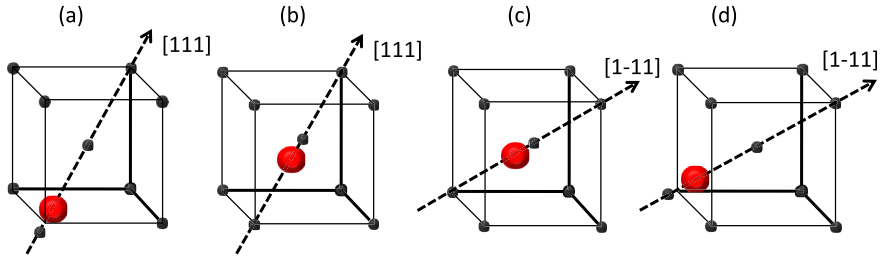

Fig. 4. Migration path of <111> solute interstitials (a red large sphere); the transformation from (a) to (b) shows a jump to a first nearest neighboring position; the transformation from (b) to (c) shows a rotation; the transformation from (c) to (d) again shows a jump to a first nearest neighboring position. (For interpretation of the references to colour in this figure legend, the reader is referred to the web version of this article.)

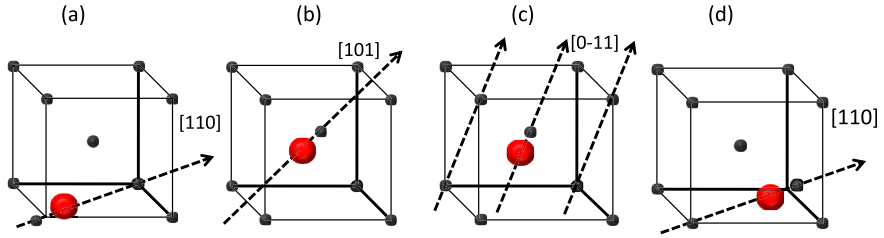

Fig. 5. Migration path of <110> solute interstitials (a red large sphere): Solute atom at (0,0,0) shown in (a) can jump either to (1/2, 1/2, 1/2) or (1/2, 1/2, −1/2); (b) shows a configuration after the jump to (1/2, 1/2, 1/2); the transformation from (b) to (c) shows a pure rotation; the transformation from (c) to (d) again shows a jump to a first nearest neighboring position. (For interpretation of the references to colour in this figure legend, the reader is referred to the web version of this article.)

an Os-interstitial (<110> dumbbell), respectively; one of these becomes an initial state of each AKMC run, and these interstitial atoms are allowed to migrate in the simulation box. We impose the periodic boundary conditions for the three directions that the dumbbell escapes from the face opposing that which it enters.

To push the clock forward, the event-driven algorithm is used, i.e., the following steps are iterated: (a) Occurrence probabilities of all the considered events are calculated on the basis of the current atomic configuration in the simulation box; (b) an event is selected randomly where the selection probability is proportional to the occurrence probability of each event; (c) the selected event is executed and the atomic configuration is updated; (d) the time advances by δt;

$$\delta t = -\frac{\log r}{k_{tot}}, \tag{1}$$

where k_{tot} is the sum of probabilities of all possible events; r is a uniform random number in the range of $0 \leq r < 1$. Each event probability is given by $\nu e^{-E_a/kT}$, where ν is the attempt frequency, and we adopt $\nu = 10^{13}$ [/s] for all events considered; k is the Boltzmann constant; T is the absolute temperature. See, for example [23], for more detail of the event-driven algorithm. Separation of the W–Re/W–Os mixed dumbbell into a substitutional solute atom and an SIA is possible in actual W crystals (see their binding energy values in Table 2), but we ignore these events; Re substitutional and Os substitutional caused by the dissociation can migrate via the vacancy mode, but as mentioned above the present study aimed at investigating the migration of solute atoms via interstitial mode, so the migrations of these products have not been included in our AKMC setting.

We estimate diffusivities of the solute atoms by applying the well-known Einstein's equation:

$$D = \frac{\left\langle \overline{R}^2 \right\rangle}{6t}, \tag{2}$$

where D is the diffusivity of the solute interstitials; $\overline{R}$ is the displacement of the interstitials during a period of t. We slightly modified Eq. (2) so that each trajectory, indexed by i, includes exactly 500 jumps;

$$D = \frac{1}{N}\sum_{i=1}^{N}\frac{\overline{R}_i^2}{6t_i}, \tag{3}$$

where N is the population of the trajectory ensemble; we set $N = 1000$. Accordingly, we collected 1000 trajectories for each case.

To conduct the above numerical analyses, we developed an AKMC code utilizing a kinetic Monte Carlo development tool called Programming Adaptable KMC Software Suite (PAKSS). PAKSS is written in C++ language and, by exploiting the polymorphism functionality of object-oriented programming, it has been successfully supplying templates for various KMC codes, such as an AKMC used in Ref. [18] and object kinetic Monte Carlo codes used in Refs. [24,25]. A project converting PAKSS to open-source software is in progress.

3. Results and discussion

Using the AKMC with the parameters mentioned in the previous section, we let an inserted interstitial migrate at a constant temperature T and recorded many trajectories of the interstitials; typical ones are displayed in Figs. 6–8 at $T = 1023^\circ$ K. This temperature is the same as that used in a recent experimental study [26]. In each case, an interstitial atom is inserted at the center of the simulation box, i.e. at the point of $x = y = z = 0$. We notice that the

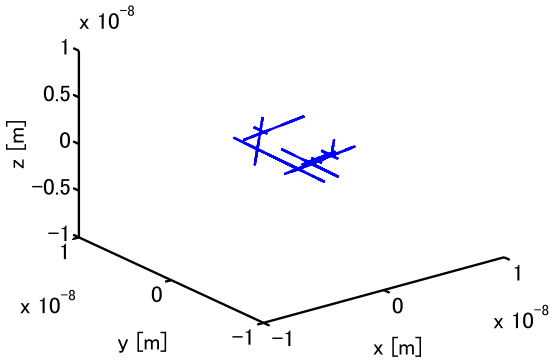

Fig. 6. A trajectory of an SIA given by a KMC run.

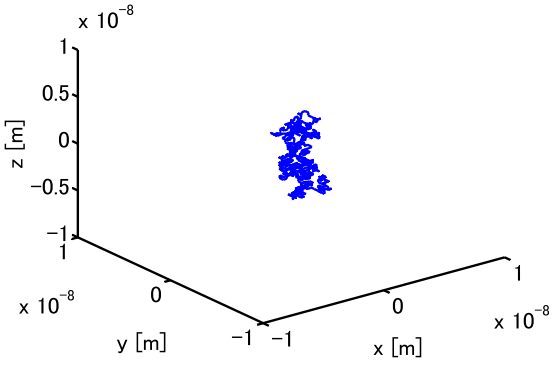

Fig. 7. A trajectory of a <111> W–Re mixed dumbbell given by a KMC run.

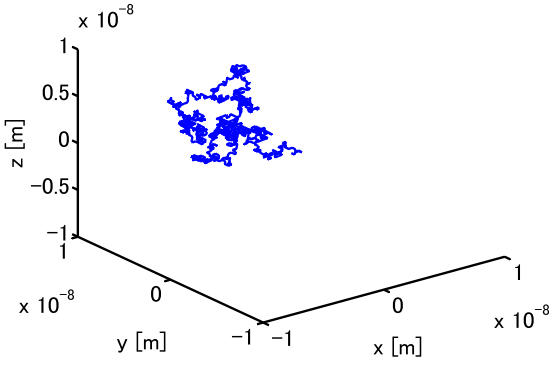

Fig. 8. A trajectory of a <110> W–Os mixed dumbbell given by a KMC run.

trajectory for the SIA in Fig. 6 is composed of one-dimensional motions with intermittent changes of direction, while the trajectories for the Re-interstitial and the Os-interstitial look like three-dimensional random walks; the results here agree with the expectation from the *ab initio* results given in Ref. [19]. By using Eq. (3) we evaluated the diffusivities of Re-interstitial and Os-interstitial atoms at various Ts as given in Fig. 9. The figure contains corresponding analytical values of vacancy-like spherical species, as given by

$$D = \frac{z\nu\delta^2}{6}e^{-E_m/kT}, \tag{4}$$

where z is the number of the first nearest neighbors (=8); δ is the distance to the first nearest neighbors ($= 0.5\sqrt{3}a_0$); E_m is the migration energy barrier given in Table 3. As shown in Fig. 9, the

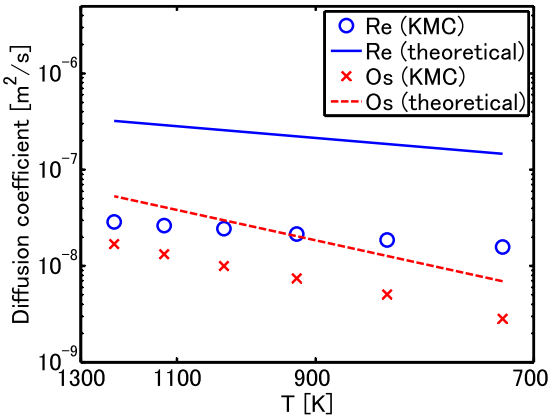

Fig. 9. Diffusivity of Re- and Os-interstitials vs. temperature.

diffusivities of vacancy-like spherical species are significantly larger than those given by the AKMC. This clearly indicates that the migration of W–Re and W–Os dumbbells cannot be modeled by Eq. (4): These dumbbells cannot be simplified as spherical objects and ought to be treated as non-spherical defects having an attribution of direction, even though their trajectories look three-dimensional as seen in Figs. 7 and 8. This is a noteworthy result deduced from the current study.

An important suggestion indicated by the previous *ab initio* study in Ref. [19] is that migration of any stable mixed dumbbell, in general, is strongly influenced by its rotation energy barrier. To verify this notion, we calculated diffusivities of <111> and <110> mixed dumbbells as a function of rotation barrier. For this purpose, we adopted the values of the other event parameters as given previously for the artificial <111> W–Re dumbbells and <110> W–Os dumbbells, while applying various values for their respective rotation energy barriers. Results given in Fig. 10 show that, for both types of mixed dumbbells at 1023° *K*, the diffusivity clearly decreases as the rotation energy barrier increases. In the case of the artificial <111> mixed dumbbell, the reason for this trend is obvious, i.e. rotation events are necessary for a Re-interstitial to escape from the trap between two neighboring W atoms, as mentioned above. For the <110> mixed dumbbells, the migration is still possible without the pure rotation, but possible migration paths are restricted without the pure rotation as implied by Fig. 5. The results in Fig. 10 indicate that frequent pure rotation events

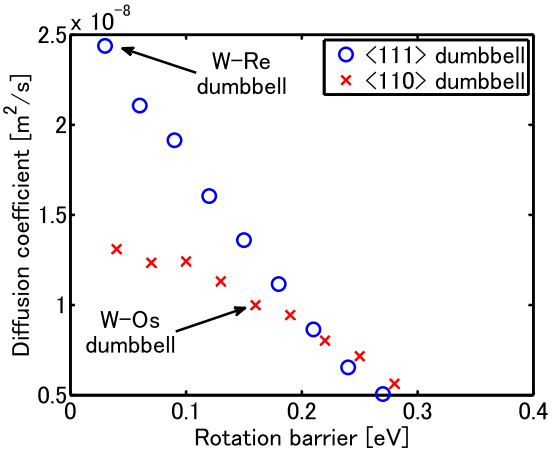

Fig. 10. Diffusivity of mixed dumbbells vs. their rotation barriers at $T = 1023°$ *K*.

strongly enhance the rate of migration of <111> and <110> mixed dumbbells in general.

In addition to RIP, experimental studies [5,9,13] revealed another radiation effect in W–Re and W–Os alloys, that is, the addition of Re or Os to pure W causes suppression of void growth. Voids in solid materials cause not only swelling but also hardening, because such voids also become obstacles for dislocation motions. So far, there is no clear explanation of how this suppression of void growth occurs. Under neutron irradiation, a primary knock-on atom (PKA) produces Frenkel pairs or a cascade of atomic displacements. In the case of pure W, surviving SIAs in the displacement have one-dimensional motion, while in W–Re alloys, surviving SIAs are likely to encounter a nearby Re substitutional atom and form a W–Re mixed dumbbell. This can experimentally recognized as the decrease in the mobility of interstitial atoms when Re is added to pure W [27]. As revealed above, W–Re mixed dumbbells have a larger migration energy barrier.

SIAs having one-dimensional motion can encounter a vacancy only along their one-dimensional migration line, so they have greater probability of escaping from cascade-displacement influenced regions without recombination, in comparison with the mixed dumbbells that have three-dimensional motion. Molecular dynamics studies of Fe–Cu alloys [28,29] show that the solute atoms increase the migration dimension of single SIAs and SIA clusters and suggest significant influence of the migration dimension to microstructural evolution. For example, kinetic Monte Carlo studies [30,31] of annealing simulation after cascade displacements in α-Fe reveal that increasing the migration dimension of interstitial clusters, from one-dimensional to three-dimensional, decreases the number of surviving vacancies. Thus, we surmise that the probability of vacancy-interstitial recombination is increased by adding Re to pure W and that the vacancy population is decreased. Hence, the three-dimensional motion of a W–Re mixed dumbbell is likely to be a cause of the suppression of void growth in W–Re alloys. The experimental fact that void-growth suppression and RIP occur simultaneously also supports the above hypothesis that the RIP develops due to vacancy-interstitial recombination as depicted in Fig. 1. The study of this hypothesis by quantitative analyses is currently in progress.

The suppression of voids is more significant in W–Os alloys [26], and the above hypothesis can similarly be applied to W–Os alloys. As shown in Figs. 9 and 10, the migration of W–Os mixed dumbbells are slower than those of W–Re dumbbells and stay longer in a cascade-displacement influenced region. Accordingly, we presumed that an interstitial in W–Os alloys has more chance of recombining with a vacancy than has an interstitial in W–Re alloys with the same solute concentration. This could be a reason for W–Os alloys having a greater suppression of voids than do W–Re alloys. Another explanation of the greater suppression of voids in W–Os alloys is that the binding energy between an Os substitutional and an SIA is much larger than that between a Re substitutional and an SIA (See Table 2), so W–Os mixed dumbbells generally have longer lifetimes in comparison with W–Re mixed dumbbells, and interstitials in W–Os alloys have more chance of recombining with a vacancy. These presumptions, also, ought to be confirmed by some quantitative analyses.

4. Conclusions

We conducted a series of atomic kinetic Monte Carlo simulations to investigate the Re-interstitial and the Os-interstitial in W crystals, which can form stable <111> and <110> mixed dumbbells, respectively, with a W atom. Our study confirms that, instead of one-dimensional motion such as SIAs have, these mixed dumbbells

have three-dimensional motion, but this motion cannot be reduced to a simple vacancy-like diffusion: The result suggests that modeling of these dumbbell needs special care in coarser modeling studies, such as those using rate equations. We also confirmed that the low rotation energy barrier of these dumbbells is a property that is key to their migration and the concomitant emergence of RIP experimentally observed in W–Re and W–Os alloys. In addition, we gave a possible explanation for the suppression of void-growth in W–Re and W–Os alloys.

Acknowledgments

T.S. and M.Y. are supported by JSPS KAKENHI Grant Number 24561044 to conduct this work. T.S. and A.H. are supported by JSPS KAKENHI Grant Number 15K06672 to conduct this work.

Appendix A. Supplementary data

Supplementary data related to this article can be found at http://dx.doi.org/10.1016/j.jnucmat.2015.05.051.

References

[1] M. Rieth, S. Dudarev, S. Gonzalez de Vicente, J. Aktaa, T. Ahlgren, S. Antusch, D. Armstrong, M. Balden, N. Baluc, M.-F. Barthe, et al., J. Nucl. Mater. 432 (2012) 482–500.
[2] T. Noda, M. Fujita, M. Okada, J. Nucl. Mater. 258 (1998) 934–939.
[3] G.A. Cottrell, R. Pampin, N.P. Tayler, Fusion Sci. Technol. 50 (2006) 89.
[4] V. Sikka, J. Moteff, Metall. Mater. Trans. B 5 (1974) 1514–1517.
[5] J. Matolich, H. Nahm, J. Moteff, Scr. Metall. 8 (1974) 837–841.
[6] R. Williams, F. Wiffen, J. Bentley, J. Stiegler, Metall. Trans. A 14 (1983) 655–666.
[7] R. Herschitz, D.N. Seidman, Nucl. Instrum. Methods Phys. Res. Sect. B: Beam Interact. Mater. Atoms 7 (1985) 137–142.
[8] Y. Nemoto, A. Hasegawa, M. Satou, K. Abe, J. Nucl. Mater. 283 (2000) 1144–1147.
[9] A. Hasegawa, T. Tanno, S. Nogami, M. Satou, J. Nucl. Mater. 417 (2011) 491–494.
[10] D. Armstrong, P. Edmondson, S. Roberts, Appl. Phys. Lett. 102 (2013), 251901–251901.
[11] B. Ralph, D. Brandon, Philos. Mag. 8 (1963) 919–934.
[12] A. Taylor, B. Kagle, N. Doyle, J. Less Common Metals 3 (1961) 333–347.
[13] M. Fukuda, T. Tanno, S. Nogami, A. Hasegawa, Mater. Trans. 53 (2012) 2145–2150.
[14] G. Martin, Phys. Rev. B 21 (1980) 2122.
[15] R. Cauvin, G. Martin, Phys. Rev. B 23 (1981) 3322.
[16] P. Krasnochtchekov, R. Averback, P. Bellon, JOM 59 (2007) 46–50.
[17] A.V. Barashev, Philos. Mag. 85 (2005) 1539–1555.
[18] K. Ebihara, T. Suzudo, M. Yamaguchi, Y. Nishiyama, J. Nucl. Mater. 440 (2013) 627–632.
[19] T. Suzudo, M. Yamaguchi, A. Hasegawa, Model. Simul. Mater. Sci. Eng. 22 (2014) 075006.
[20] G. Kresse, D. Joubert, Phys. Rev. B 59 (1999) 1758–1775.
[21] G. Kresse, J. Furthmüller, Phys. Rev. B 54 (1996) 11169–211186.
[22] T. Suzudo, M. Yamaguchi, Submitt. J. Nucl. Mater. (2015).
[23] A.F. Voter, "Introduction to the Kinetic Monte Carlo Method," in Radiation Effects in Solids, Springer, 2007, pp. 1–23.
[24] Y. Abe, T. Suzudo, S. Jitsukawa, T. Tsuru, T. Tsukada, Fusion Sci. Technol. 62 (2012) 139–144.
[25] T. Suzudo, S.I. Golubov, R.E. Stoller, M. Yamaguchi, T. Tsuru, H. Kaburaki, J. Nucl. Mater. 423 (2012) 40–46.
[26] T. Tanno, A. Hasegawa, M. Fujiwara, J.-C. He, S. Nogami, M. Satou, T. Shishido, K. Abe, Mater. Trans. 49 (2008) 2259.
[27] K. Wilson, M. Baskes, D. Seidman, Acta Metall. 28 (1980) 89–102.
[28] J. Marian, B. Wirth, J. Perlado, G. Odette, T.D. de la Rubia, Phys. Rev. B 64 (2001) 094303.
[29] J. Marian, B. Wirth, A. Caro, B. Sadigh, G. Odette, J. Perlado, T.D. de la Rubia, Phys. Rev. B 65 (2002) 144102.
[30] T. Suzudo, S.I. Golubov, R.E. Stoller, Prog. Nucl. Sci. Technol. 2 (2011) 56–63.
[31] H. Xu, Y.N. Osetsky, R.E. Stoller, J. Nucl. Mater. 423 (2012) 102–109.